33RD CONGRESS
OF THE INTERNATIONAL COUNCIL
OF THE AERONAUTICAL SCIENCES
STOCKHOLM, SWEDEN, 4-9 SEPTEMBER, 2022

ICAS 2022 SWEDEN

STABILTY AND TRANSITION OF A LAMINAR SEPARATION BUBBLE SUBJECTED TO FREESTREAM TURBULENCE

Thomas Jaroslawski*[1], Olivier Vermeersch[1], Jean-Marc Moschetta[2], Maxime Forte[1] & Erwin Gowree[2]

[1] Dept. of Multi-Physics for Energetics, ONERA, Toulouse, France.
[2]Dept. of Aerodynamics and Propulsion, ISAE-SUPAERO, Toulouse, France.
**thomas.jaroslawski@onera.fr

Abstract

Experiments were conducted to study the transition and flow development in a laminar separation bubble (LSB) formed on an aerofoil. The effects of a wide range of freestream turbulence intensity ($0.15\% < Tu < 6.26\%$) and streamwise integral length scale ($4.6mm < \Lambda_u < 17.2mm$) are considered. The coexistence of a modal instability due to the LSB and a non-modal instability caused by streaks generated by freestream turbulence is observed. The presence of streaks in the boundary layer modifies the mean flow topology of the bubble. These changes in the mean flow field result in the modification of the convective disturbance growth, where an increase in turbulence intensity is found to dampen the growth of the modal instability. For a relatively fixed level of Tu, the variation of Λ_u has modest effects, however, a slight advancement of the non-linear growth of disturbances and eventual breakdown with the decrease in Λ_u is observed. The data shows that the streamwise growth of the disturbance energy is exponential for the lowest levels of freestream turbulence and gradually becomes algebraic as the level of freestream turbulence increases. Once a critical turbulence intensity is reached, there is enough energy in the boundary layer to suppress the LSB, which in turn, results in the non-modal instability taking over the transition process. Linear stability analysis is conducted in the fore position of the LSB, and accurately models unstable frequencies and eigenfunctions for configurations subjected to levels of turbulence intensity levels up to 3%.

Keywords: Laminar Separation Bubble; Freestream turbulence; Stability ; Transition; Integral Length scale

Introduction

For boundary layer flows at low Reynolds numbers viscous effects are significant, such that the presence of a strong enough adverse pressure gradient can cause a laminar boundary layer to separate from the wall. As a result of boundary layer separation, the detached laminar shear layer undergoes the transition to turbulence. These types of flows are common in engineering applications such as micro-aerial vehicles [Jaroslawski et al., 2022a,b]. The transition process in the separated shear layer involves the amplification of the convective (Kevin Helmholtz) instability in the fore portion of the bubble and is modeled well with Linear Stability Theory. The effects of freestream turbulence (FST) and the integral length scale on boundary layer transition have not been addressed to the same extent as for attached boundary layers (Fransson and Shahinfar [2020]), notably, there is a lack of experimental results on the role of the integral length scales. Recently, Istvan and Yarusevych [2018] experimentally investigated the effects of FST on an LSB over a NACA0018 aerofoil using Particle Image Velocimetry (PIV). They found that increasing the level of FST decreases in the chordwise length of the LSB due to a downstream shift of the separation point and an upstream shift of the reattachment point. They concluded that the maximum spatial amplification of disturbances in the separated shear layer decrease with increasing Tu, implying that the larger initial disturbances are solely responsible for the earlier transition and reattachment. At levels of FST of 1.99%, streamwise

streaks were found upstream and inside the bubble, similar to early experiments by Häggmark et al. [2000], signifying the onset of turbulence induced or "bypass" transition, and suggesting that the dominance of this transition mechanism could eliminate the bubble. Hosseinverdi and Fasel [2019] used direct numerical simulations (DNS) to investigate the role of isotropic FST on an LSB and reported Klebanoff modes upstream of the separation location. It was suggested that the boundary layer transition process consisted of two mechanisms. The first, low-frequency Klebanoff modes caused by the FST, and the second, the FST amplifying frequencies of the order of the shedding the FST enhancing the initial levels of instability waves in the frequency range of the KH instability, albeit at a lower amplitude than the Klebanoff modes. Depending on the level of FST either one or both of these mechanisms would dominate the transition process.
The objectives of the current experimental investigation are to study the impact of freestream turbulence and integral length scale on the convective growth of energy disturbances and transition mechanisms in an LSB.

Experiments

The experiments were conducted at atmospheric conditions in the ONERA Toulouse TRIN 2 subsonic wind tunnel. The maximum freestream turbulence level (measured near the leading edge of the aerofoil, cf. Fig. 1a) in the test section with the aerofoil mounted was found to be below 0.15 %. The freestream velocity was fixed at $U_\infty \cong 6m/s$ for all test configurations, corresponding to a chord-based Reynolds number, $Re_c = U_\infty c/\nu$ of 125000. The angle of attack, AoA, was fixed to a value of 2.3° throughout all the experiments. Velocity measurements are acquired using a Dantec Dynamics Streamline Pro system with a 90C10 module and a 55P15 boundary layer probe mounted on a two-dimensional traverse, at a sampling frequency of 25 kHz. Freestream turbulence measurements were conducted using a 5 μm Dantec 55P51 X-Wire probe. Freestream turbulence is generated in a controlled manner using a variety of regular and fractal grids (refer to Fig. 1 b,c) set up in a way such that turbulence interacting with the bubble would be approximately isotropic and homogeneous. The evolution of the grid-generated turbulence was characterised before the leading edge and above the aerofoil. Infrared Thermography measurements were also conducted to validate the spanwise flow homogeneity of the bubble (which are not presented in the present paper). The experimental setup is presented in Fig. 1a. The uncertainty in hotwire measurements was estimated to be less than 3%, for $U/U_\infty > 0.2$, and the uncertainty in the hotwire positioning is estimated to be less than 0.05 mm. The use of HWA in the study of LSBs is fraught with difficulty. In particular, the mean velocity measurement cannot detect the reverse flow region in the LSB. Nevertheless, as demonstrated by Boutilier and Yarusevych [2012], HWA can be used to study the transition mechanisms in an LSB.

Results

Mean Flow Field

The mean streamwise velocity and u_{rms} contours (which are composed of 21 streamwise velocity profiles separated by $0.025c$ in the chordwise direction) are presented in Fig. 2a and show the presence of an LSB that extends from x_S/c = 0.375 $\pm$ 0.05 to x_S/c = 0.700 $\pm$ 0.025 for the natural case. In the presence of freestream turbulence forcing the mean flow topology of the LSB changes, in particular, a slight delay of boundary layer separation is observed, the height decreases significantly and the mean transition position advances upstream as can be observed in Fig. 2b. At the highest level of Tu (Fig. 2c), no LSB is observed as there is enough energy injected from the freestream turbulence into the boundary layer to suppress the laminar separation. The measurements, in accordance with previous studies [Istvan and Yarusevych, 2018, Simoni et al., 2017, Hosseinverdi and Fasel, 2019], show that with the increase of Tu, the streamwise extent of the separation bubble is reduced. This is a result of an earlier onset of pressure recovery, caused by the shear layer transitioning in the aft position of the LSB.

Power spectral density

The power spectral density (PSD) of the streamwise velocity fluctuations was calculated for each configuration, with the chordwise evolution presented in Fig. 3. In the cases where an LSB was

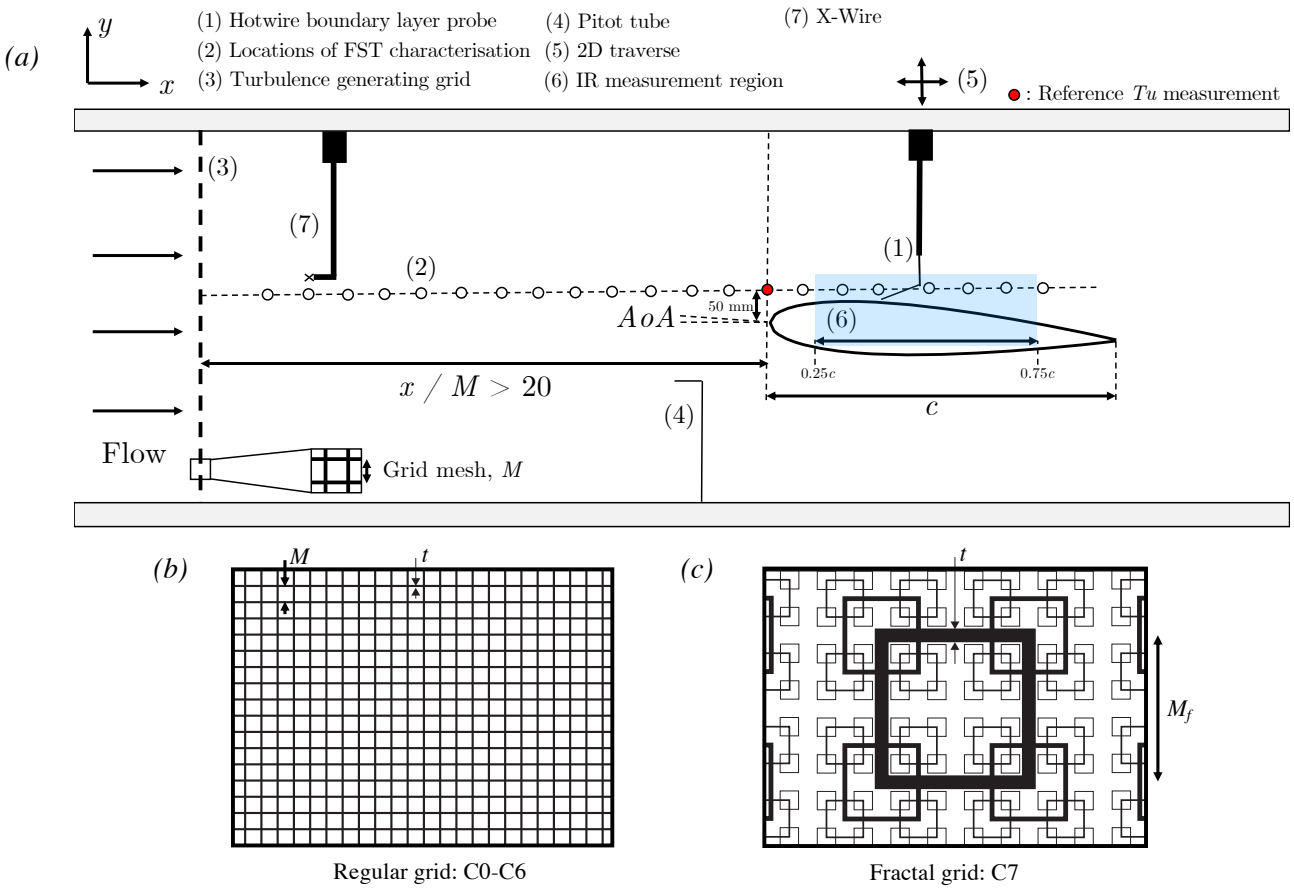

Figure 1 – a)Experimental Setup. (b) Schematic of regular grid (configs. C0-C6) and (b) fractal grid (config. C7)

present, the PSD exhibits a characteristic frequency band which amplified downstream (cf. Fig. 3a-g). When the LSB was subjected to FST the chordwise development and distribution of the spectra is significantly modified. First, the unstable frequency band is broadened, which is a consequence of significant energy content within a broader range of frequencies in the FST, resulting in measurable velocity fluctuations over a broader frequency range earlier upstream. Second, increasing the freestream turbulence level results in the unstable frequency band being slightly shifted to a higher frequency range compared to the natural case. For example, increasing the freestream turbulence level from the baseline to a value of $Tu = 1.23\%$, results in the frequency band being shifted from $110 - 150Hz$ to $180 - 220Hz$ (cf. Fig. 3a and d). Referring to Fig. 3a-g, the unstable frequency band is propagated upstream of the separation point and is due to the streamwise oscillation of the separation bubble. The highest frequency wave packet is found to occur in the highest Tu case which was $255 - 295Hz$, wherein the highest cases ($Tu > 4\%$, Fig. 3h,i) no clear frequency band is observed and is thought to be due to the LSB not being present anymore, inferring a change in the instability mechanism. The frequency shift of the wave packet is attributed to the decreased streamwise length and height of the LSB and has been observed in Hosseinverdi and Fasel [2019]. Current results suggest that in the configurations that are subjected to a turbulence intensity of $Tu < 3\%$ the harmonic of the frequency band is still observed, which could suggest that in the presence of moderate levels of FST the secondary instability of the primary modal instability could still be present. The current results also indicate that if the Tu is increased to a certain level, the harmonic of the wave packet is barely noticeable (cf. Fig.3g), suggesting that there is a certain threshold of FST forcing which will "bypass" the secondary instability, which will still exist in moderate cases, and in accordance with the numerical simulations of Li and Yang [2019]. Additionally, as in Balzer and Fasel [2016], possible harmonics are observed in the spectra for the LSB subjected to FST. The impact of the integral length scale has a negligible effect on the unstable frequency range of the wave packet.

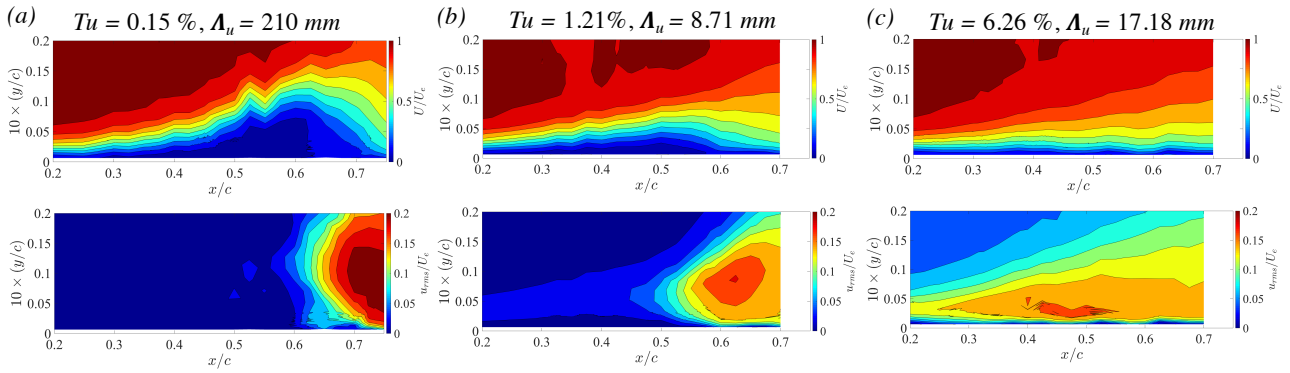

Figure 2 – Contours of the mean streamwise velocity (U) and the r.m.s of the fluctuating streamwise velocity (u_{rms}) (a) 0.15% (b) 1.21% and (c) 6.28%.

Pauley et al. [1990] proposed a scaling of the most unstable frequency in an LSB, in the form of a Strouhal number defined as:

$$St_{\delta_2} = \frac{F\delta_{2,s}}{U_{e,s}} \tag{1}$$

where F is the most amplified frequency observed in the experiment, $\delta_{2,s}$ and $U_{e,s}$ are the momentum thickness and boundary layer edge velocity at separation, respectively. Inspired by the analysis of Rodríguez and Gennaro [2019] and Rodríguez et al. [2021], who compared the value of the St_{δ_2} for past experiments on LSBs, Fig. 1 compares the value of St_{δ_2} as a function of Tu (for the cases where an LSB was observed). In the configuration where the laminar separation bubble is subjected to no additional freestream turbulence, $St_{\delta_2} = 0.0062$, compared to the 'universal' $St_{\delta_2} = 0.0069$ proposed by Pauley et al. [1990] for 2D numerical simulations of a laminar separation bubble. However, increasing the Tu causes St_{δ_2} to increase, when compared to the baseline case, approaching values closer to what was proposed by Rodríguez et al. [2021] of $St_{\delta_2} = 0.01 - 0.012$ for a bubble acting as a global oscillator. Data from Istvan and Yarusevych [2018] also suggest this effect and Pauley et al. [1990] found that $St_{\delta_2} = 0.0124 - 0.0136$ in 3D unforced numerical simulations twice as large of what was observed for 2D simulations. Therefore, the increased values of St_{δ_2} suggest that the presence of freestream turbulence (or increased levels of forcing) could favour the inherent three-dimensional nature of the transition process in the LSB. Furthermore, Rodríguez and Gennaro [2019] found that increasing the recirculating velocity in the bubble, increased the values of St_{δ_2} which could manifest here as well as the LSBs subjected to FST are smaller in size for the same convective velocity, which could result in larger levels of re-circulation inside the bubble. Finally, discrepancies in the values can be associated with the fact that the experiments were conducted on both flat plates (with imposed pressure gradients) and aerofoils, different Reynolds numbers, the surface finish of the model, and the inherent uncertainty in the various measurement techniques.

Disturbance energy growth

The effect of increasing the level of Tu on the chordwise evolution of the disturbance energy growth ($E = u_{rms}^2/U_e^2$) is presented in Fig. 4a, where the trend of disturbance growth gradually changes from exponential, at lower levels of Tu, to algebraic for the more extreme Tu levels, where energy saturation is observed earlier. Algebraic or transient growth is associated with a non-modal instability, commonly due to streaks in boundary layer flows subjected to elevated levels of freestream turbulence ($Tu > 1\%$) and has been well documented for zero-pressure gradient attached boundary layers [Matsubara and Alfredsson, 2001]. These different energy growth behaviours suggest that different instability mechanisms are present in the flow, and their contribution to the transition process depends on the level of the freestream forcing.

The gradual reduction in the slope of the chordwise energy growth with increasing Tu would suggest that the non-modal instabilities become more dominant, which can be thought of as competing with the modal instabilities which grow exponentially. Once the turbulence forcing reaches a critical level,

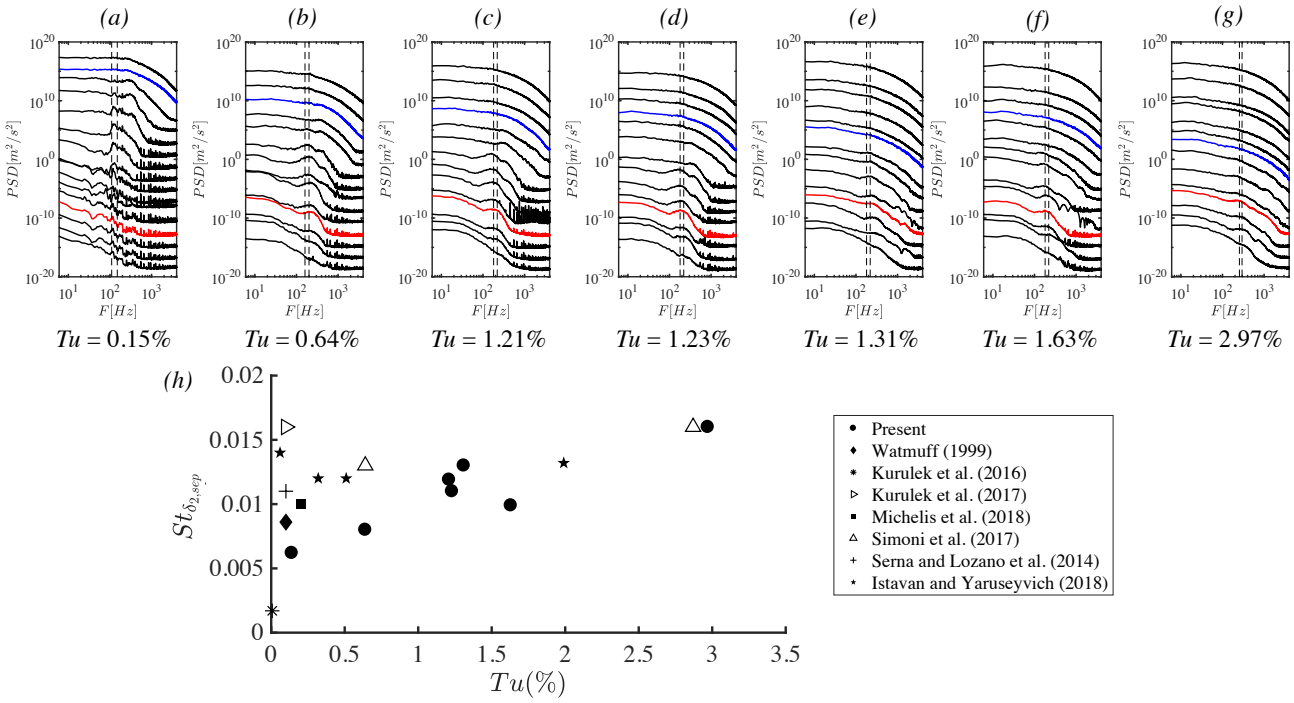

Figure 3 – a-g) Chordwise evolution of the Power Spectral Density (PSD) at the maximum location of u_{max} inside the boundary layer for each configuration. Where the frequency bands correspond to the vertical dashed lines which indicate the most amplified frequency band used in the stability analysis in the following section. Red and blue curves denote x_S and x_R, respectively. NB: Spectra are separated by an order of magnitude for clarity. h) The dimensionless frequency, St_{δ_2}, plotted against the turbulence intensity, Tu, for the present results and experimental data from the literature.

the excited streaks in the boundary layer are too energetic to allow the flow to separate, resulting in the elimination of the modal via the non-modal instability. Damping of the modal disturbance growth is attributed to the mean flow deformation due to the influence of freestream turbulence. In other words, external freestream turbulence forcing reduces the size of the separation bubble, such that the region of instability growth is brought closer to the wall, resulting in damping effects of the disturbances in the shear layer.

The impact of the integral length scale for a relatively constant Tu level on the disturbance growth is presented in Fig. 4c, suggesting that the effect of the integral length scale on the growth of disturbances in the LSB is very modest. Achieving constant levels of Tu with a varying Λ_u is an experimental challenge, as shown by Fransson and Shahinfar [2020]. In the present work, three cases that have a very small variation in Tu and a larger variation in Λ_u are investigated. It is observed that an increase in Λ_u at the leading edge of the aerofoil for an almost constant Tu appears to delay the growth and eventual saturation and breakdown of the disturbances. This is in agreement Breuer [2018], who suggested that the smaller scales were closer to that of the shear layer, resulting in the receptivity of the boundary layer to increase. Hosseinverdi and Fasel [2019] briefly suggested that the integral length scales ranging from $0.9\delta_1$ to $3\delta_1$ had little effect on the energy growth relative to the Tu, which is observed in the experimental results here. Furthermore, a smaller integral length scale resulted in a higher initial level of disturbance energy in the boundary layer and has been also observed by Hosseinverdi [2014], however in their work, the saturation of the energy growth was found to be independent of Λ_u. Breuer [2018] conducted an LES on an aerofoil and found that a reduction of the integral length scale advanced the transition position, suggesting that smaller scales closer to that of the shear layer resulted in the receptivity of the boundary layer increase. Based on the experimental observations here and past numerical simulations, an effect of the integral length scale could be present and further investigation is warranted. However, the effect will likely be small compared to the Tu, in light of the results here and Hosseinverdi and Fasel [2019].

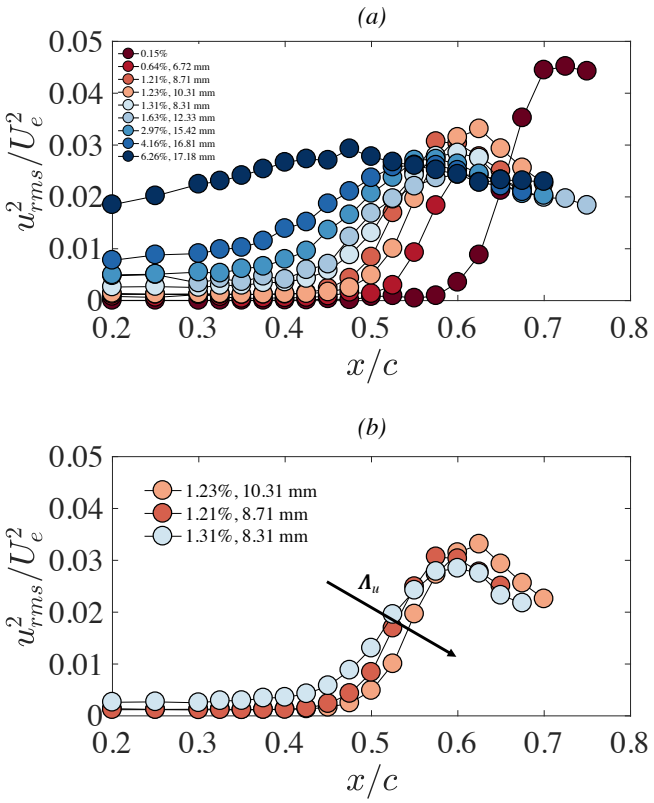

Figure 4 – The disturbance energy growth for a) integrated over the entire energy spectrum and b) configurations with are relatively fixed Tu and varying Λ_u.)

Linear Stability Analysis

Linear Stability Theory (LST) models the amplification of small amplitude disturbances [Schmid and Henningson, 2000] and has been employed to study the convective streamwise amplification of disturbances in the LSB. The Orr-Sommerfeld given by Eq. 2, can reliably predict the primary amplification of instability waves for parallel flows and in the fore position of an LSB [Kurelek et al., 2018].

$$\left(U-\frac{\Omega}{\alpha}\right)\left(\frac{d^2\tilde{v}}{dy^2}-\alpha^2\tilde{v}\right)-\frac{d^2U}{dy^2}\tilde{v}=-\frac{iU_e\delta_1}{\alpha Re_{\delta_1}}\left(\frac{d^4\tilde{v}}{dy^4}-2\alpha^2\frac{d^2\tilde{v}}{dy^2}+\alpha^4\tilde{v}\right) \tag{2}$$

where Re_{δ_1} is the Reynolds number based on displacement thickness, $\tilde{v}$ is the wall-normal perturbation, Ω is the angular frequency and the complex wavenumber is defined as $\alpha=\alpha_r+i\alpha_i$, where i is the imaginary unit. When $\alpha_i>0$ the disturbance is attenuated and amplified when $\alpha_i<0$.

Calculations were conducted using ONERA's in-house stability code, where a spatial formulation of the problem is employed [Schmid and Henningson, 2000], such that Ω is defined and the eigenvalue problem is solved for α, therefore modeling the convective amplification of single frequency disturbances. Equation 2 is solved numerically using Chebyshev polynomial base functions and the companion matrix technique to treat eigenvalue non-linearity [Bridges and Morris, 1984].

The mean streamwise velocity profiles at discrete streamwise locations are used as input for the LST calculations, making the analysis local, with the same methodology employed by Yarusevych and Kotsonis [2017] and Kurelek et al. [2018]. In the stability analysis, the higher-order spatial gradients are highly sensitive to noise, therefore hyperbolic tangent fits are used for the calculations. This method has been shown to provide accurate linear stability predictions on HWA velocity profiles of separated shear layers [Boutilier and Yarusevych, 2012]

A measure of the amplitude growth is quantified from LST through the computation of amplification factors and will be referred to as the $N-$factor hereinafter. The $N-$factor as a function of streamwise position (x) and frequency (F) from LST calculations and is quantified by integrating α_i for the most amplified frequency in the positive $x-$direction:

$$N(x,F) = \int_{x_{cr}}^{x} -\alpha_i \, dx \tag{3}$$

where x_{cr} is the critical abscissa and corresponds to the location at which a perturbation at a frequency of Ω is first amplified. The location of x_{cr} is upstream of the hot wire measurement region and therefore cannot be determined directly. However, as demonstrated by Jones et al. [2010], Kurelek et al. [2018], Yarusevych and Kotsonis [2017] and Kurelek [2021], in the fore portion of the LSB the streamwise evolution of α_i can be approximated by a second-order polynomial. For example, Kurelek [2021] (HWA, Ch. 6) and Kurelek et al. [2018] (PIV) demonstrated that the $(-\alpha_i)$ obtained from LST calculations, for four velocity profiles before and after the separation position could be used in the interpolation. Considering this, x_{cr} can be determined by extrapolating the fit to $\alpha_i = 0$. Experimentally, the $N-$factor is calculated as $N(x) = ln(A(x)/A_{cr})$, where $A(x)$ denotes the maximum disturbance amplitude in the boundary layer for a given frequency band (band-pass filtered u_{rms}) and A_{cr} denotes the initial disturbance amplitude that becomes unstable. A direct comparison of $N-$factor obtained from LST and experiment is not possible since, experimentally, the initial disturbance amplitude is not known and likely to be too small to be measured, only being detected well downstream of x_{cr}. Nevertheless, following Schmid and Henningson [2000], $N-$factors are matched at a reference location where the disturbance amplitude reaches $0.005U_\infty$, consequently allowing for an estimate of A_{cr} for a given frequency band.

In the baseline configuration (cf. Fig. 5a, NB. the figures show both the energy in the spectra and α_i and direct comparisons between their magnitudes are not to be made, only the frequencies at which the largest magnitudes occur), the overlaid plot between PSD and α_i show that LST is capable of predicting the most amplified frequencies from experiment, with acceptable accuracy (10% difference). For example, Kurelek et al. [2018] and Yarusevych and Kotsonis [2017] found a difference of 17%, while stating this to be an acceptable range. The validity of the LST predictions is further supported by a comparison with experimental $N-$factors (cf. Fig. 7a), which reveals that the linear growth of disturbances is captured between $0.475 < x/c < 0.525$, comparable to the same analysis by Kurelek et al. [2018] who found LST to accurately capture the growth of disturbances between $0.42 < x/c < 0.46$ in the experiment. Furthermore, the downstream saturation of the experimental $N-$factors, begins to deteriorate the agreement between LST due to non-linear effects becoming significant. The eigenfunction of the most amplified frequency predicted by LST is presented in Fig 6a, and is in acceptable agreement with the experiment for filtered fluctuating streamwise velocity profile in the wall-normal direction, for the most amplified frequency band. The eigenfuction exhibits two distinct peaks at approximately $y/\delta_1 = 1$, corresponding roughly to the inflection point and $y/\delta_1 = 0.3$, which is indicative of a viscous modal instability [Veerasamy et al., 2021]. Rist and Maucher [2002] showed that LSBs with smaller wall-normal distances could exhibit a viscous modal instability. Therefore, based on the agreement seen in unstable frequencies, eigenfunctions, and amplification rates (Figs. 5a, 6 and 7a), it is established that the employed LST analysis is justified for determining stability characteristics in the fore portion of the LSB.

Co-existence of a modal and a non-modal instability

The disturbance profiles in the aft position of the bubble presented in Fig. 8b,c, strongly suggest the existence of the non-modal growth or streaks as the profiles exhibit self-similar behaviour with the optimal disturbance profiles from the theoretical work of Luchini [2000], with the maximum value of u_{rms} occurring near $y/\delta_1 = 1.3$ for all configurations with $Tu > 1\%$. The current results demonstrate self-similarity of the disturbance profiles over most of the boundary layer. These observations made in Figs.6 and 8 imply the co-existence of both modal and non-modal instability mechanisms, experimentally confirming the observations made by Hosseinverdi and Fasel [2019]. In contrast, in configurations where the $Tu < 1\%$ (refer to Fig. 8a), wall-normal disturbance profiles do not agree with theoretical predictions and do not exhibit the same behaviour as for configurations with $Tu > 1\%$, with the maxima of the peaks being between $y/\delta_1 = 0.3 - 0.5$, inferring that there is no formation of streaks and that only a viscous modal transition mechanism is present. The observation of damping behaviour on the disturbance growth presented in the previous section (Fig. 4) being due to the non-modal amplification of streaks is supported by the results in Fig. 8. Finally, when the bubble is

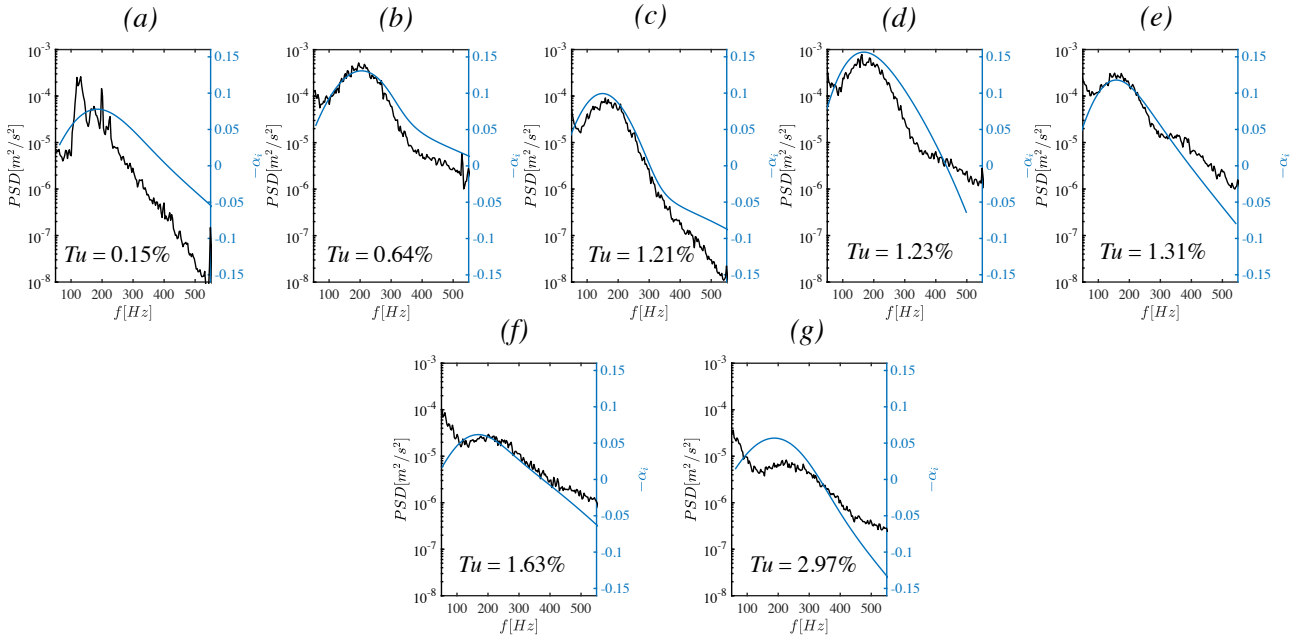

Figure 5 – Comparison between the amplified frequencies predicted by LST to the experimental spectra. NB: Two different $y-$axes for α_i and the power from the PSD, therefore direct comparisons between the two are not be made.

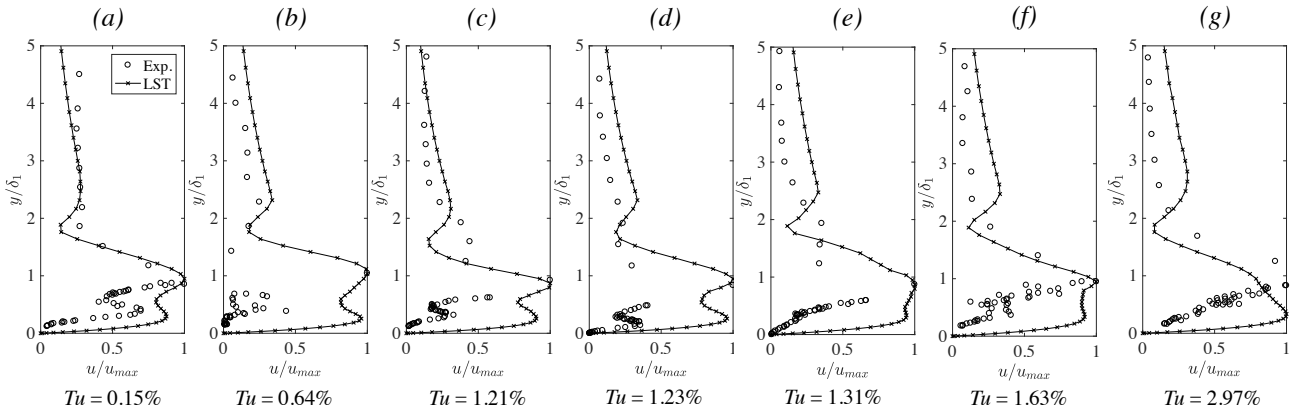

Figure 6 – Experimental filtered disturbance profiles in the wall-normal direction compared to the eigenfunction for the most amplified frequency from LST. Experimental streamwise disturbance profiles are computed by applying a bandpass filter corresponding to the lost amplified frequency band from the PSD.

subjected to a sufficient level of freestream turbulence forcing ($Tu > 3\%$, in the present configuration) the formation of an LSB is not observed in the experimental data, suggesting that there is a critical initial forcing amplitude which will generate streaks containing enough energy to suppress boundary layer separation by promoting earlier transition. Disturbance profiles (cf. Fig. 8c) are in very good agreement with the theory.

Conclusions

The present investigation examined the effects of varying the freestream turbulence intensity and integral length scale on the flow development and transition in a laminar separation bubble. The current work provides experimental evidence on the coexistence of modal and non-modal instabilities in a laminar separation bubble. It is shown, through experiment and theory, that even at relatively high/moderate turbulence intensity levels the modal instability is still operational in an LSB and the primary growth can be satisfactorily predicted with the Orr-Sommerfeld formulation. The damping of the streamwise growth of disturbances is due to the presence of streaks caused by the elevated levels

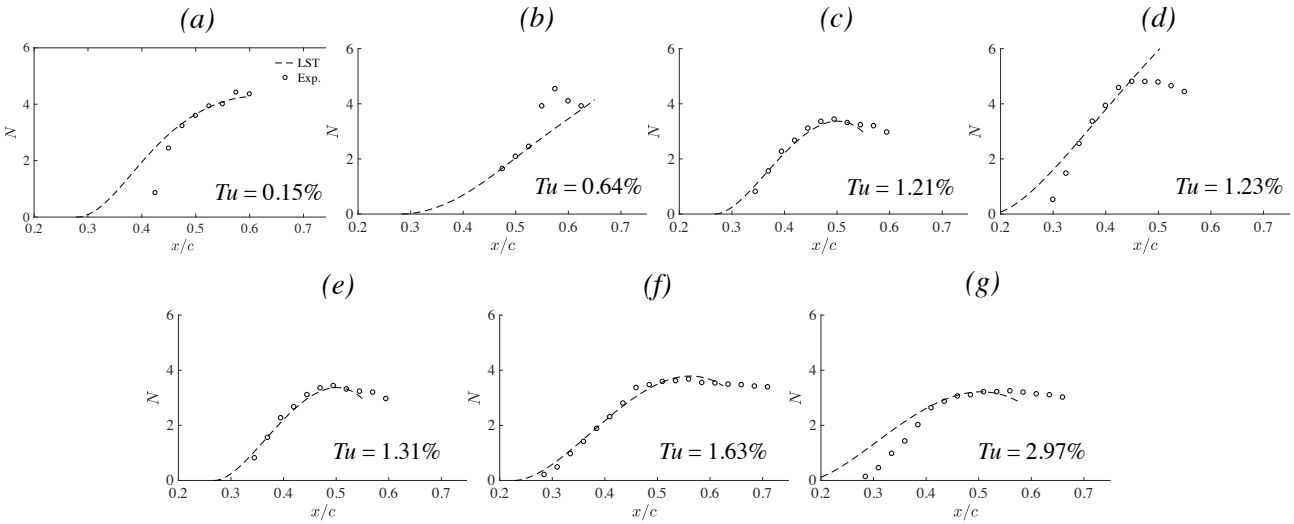

Figure 7 – Comparison of experimental (markers) LST (dashed line) predicted $N-$factors for frequencies within the excitation bands from Fig. 3 for configurations where a laminar separation bubble is present. Initial disturbance amplitudes are estimated through matching LST and experimental $N-$factors

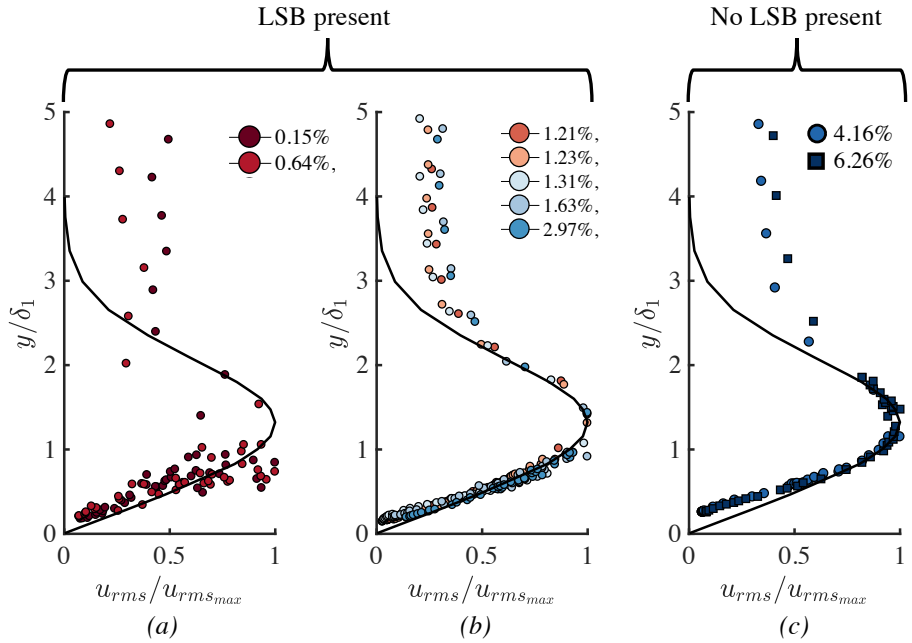

Figure 8 – Disturbance profiles for a) configurations with $Tu < 1\%$ (with LSB) b) $1\% < Tu < 3\%$ (with LSB) and c) $Tu > 3\%$ (no LSB)

of freestream turbulence, which modify the mean flow topology of the bubble through the introduction of non-modal disturbances (streaks) into the boundary layer.

References

Wolfgang Balzer and Hermann F Fasel. Numerical investigation of the role of free-stream turbulence in boundary-layer separation. *Journal of Fluid Mechanics*, 801:289–321, 2016.

Michael SH Boutilier and Serhiy Yarusevych. Separated shear layer transition over an airfoil at a low reynolds number. *Physics of Fluids*, 24(8):084105, 2012.

Michael Breuer. Effect of inflow turbulence on an airfoil flow with laminar separation bubble: An les study. *Flow, Turbulence and Combustion*, 101(2):433–456, 2018.

TJ Bridges and Philip John Morris. Differential eigenvalue problems in which the parameter appears nonlinearly. *Journal of Computational Physics*, 55(3):437–460, 1984.

Jens HM Fransson and Shahab Shahinfar. On the effect of free-stream turbulence on boundary-layer transition. *Journal of Fluid Mechanics*, 899, 2020.

CP Häggmark, Andrey A Bakchinov, and P Henrik Alfredsson. Experiments on a two–dimensional laminar separation bubble. *Philosophical Transactions of the Royal Society of London. Series A: Mathematical, Physical and Engineering Sciences*, 358(1777):3193–3205, 2000.

Shirzad Hosseinverdi. Influence of free-stream turbulence on laminar-turbulent transition in long laminar separation bubbles: Direct numerical simulations. Master's thesis, 2014.

Shirzad Hosseinverdi and Hermann F Fasel. Numerical investigation of laminar–turbulent transition in laminar separation bubbles: the effect of free-stream turbulence. *Journal of Fluid Mechanics*, 858:714–759, 2019.

Mark S Istvan and Serhiy Yarusevych. Effects of free-stream turbulence intensity on transition in a laminar separation bubble formed over an airfoil. *Experiments in Fluids*, 59(3):52, 2018.

Thomas Jaroslawski, Maxime Forte, Jean-Marc Moschetta, Gregory Delattre, and Erwin R Gowree. Characterisation of boundary layer transition over a low reynolds number rotor. *Experimental Thermal and Fluid Science*, 130:110485, 2022a.

Thomas Jaroslawski, Maxime Forte, Jean-Marc Moschetta, and Erwin Ricky Gowree. Boundary layer transition over a low Reynolds number rotor: effects of roughness and freestream turbulence. pages FP97–2022, 2022b.

LE Jones, RD Sandberg, and ND Sandham. Stability and receptivity characteristics of a laminar separation bubble on an aerofoil. *Journal of Fluid Mechanics*, 648:257–296, 2010.

John Kurelek. *The vortex dynamics of laminar separation bubbles*. PhD thesis, University of Waterloo, 2021.

John William Kurelek, Marios Kotsonis, and Serhiy Yarusevych. Transition in a separation bubble under tonal and broadband acoustic excitation. *Journal of Fluid Mechanics*, 853:1–36, 2018.

Hua J Li and Zhiyin Yang. Separated boundary layer transition under pressure gradient in the presence of free-stream turbulence. *Physics of Fluids*, 31(10):104106, 2019.

Paolo Luchini. Reynolds-number-independent instability of the boundary layer over a flat surface: optimal perturbations. *Journal of Fluid Mechanics*, 404:289–309, 2000.

M Matsubara and P Henrik Alfredsson. Disturbance growth in boundary layers subjected to free-stream turbulence. *Journal of fluid mechanics*, 430:149, 2001.

Laura L Pauley, Parviz Moin, and William C Reynolds. The structure of two-dimensional separation. *Journal of fluid Mechanics*, 220:397–411, 1990.

Ulrich Rist and Ulrich Maucher. Investigations of time-growing instabilities in laminar separation bubbles. *European Journal of Mechanics-B/Fluids*, 21(5):495–509, 2002.

D Rodríguez and EM Gennaro. Enhancement of disturbance wave amplification due to the intrinsic three-dimensionalisation of laminar separation bubbles. *The Aeronautical Journal*, 123(1268):1492–1507, 2019.

Daniel Rodríguez, Elmer M Gennaro, and Leandro F Souza. Self-excited primary and secondary instability of laminar separation bubbles. *Journal of Fluid Mechanics*, 906, 2021.

Peter J Schmid and Dan S Henningson. *Stability and transition in shear flows*, volume 142. Springer Science & Business Media, 2000.

Daniele Simoni, Davide Lengani, Marina Ubaldi, Pietro Zunino, and Matteo Dellacasagrande. Inspection of the dynamic properties of laminar separation bubbles: free-stream turbulence intensity effects for different reynolds numbers. *Experiments in Fluids*, 58(6):66, 2017.

Dhamotharan Veerasamy, Chris J Atkin, and Sathiskumar A Ponnusami. Aerofoil wake-induced transition characteristics on a flat-plate boundary layer. *Journal of Fluid Mechanics*, 920, 2021.

Serhiy Yarusevych and Marios Kotsonis. Steady and transient response of a laminar separation bubble to controlled disturbances. *Journal of Fluid Mechanics*, 813:955–990, 2017.